Direct observation of hyperfine quenching of the $2\,^3P_0$ level in heliumlike nickel

R. W. Dunford, C. J. Liu, J. Last, N. Berrah-Mansour, and R. Vondrasek
Physics Division, Argonne National Laboratory, Argonne, Illinois 60439

D. A. Church
Department of Physics, Texas A&M University, College Station, Texas 77843

L. J. Curtis
Department of Physics and Astronomy, University of Toledo, Toledo, Ohio 43606
(Received 11 February 1991)

We report a clear demonstration of the effect of hyperfine quenching of a forbidden transition by direct comparison of the lifetimes of the $2\,^3P_0$ level in the heliumlike isotopes $^{61}Ni^{26+}$ and $^{58}Ni^{26+}$. We find the quenched lifetime of the $2\,^3P_0$ level in $^{61}Ni^{26+}$ to be 470(50) ps. From this we deduce the $2\,^3P_0$–$2\,^3P_1$ energy splitting to be 2.33(15) eV. We also report a measurement of the lifetime of the $2\,^3P_2$ level in $^{58}Ni^{26+}$, which is found to be 70(3) ps.

One of the most interesting phenomena in the theory of highly forbidden transitions is the effect of hyperfine quenching, whereby mixing by the hyperfine interaction can significantly alter the lifetimes of the levels. The phenomenon was first discussed by Bowen [1] in 1930, who pointed out that the substantial strength that was observed in the $6s^2\,^1S_0$–$6s6p\,^3p_2$ line at 2270 Å in the spectrum of Hg I was primarily due to $E1$ radiation caused by coupling with the nuclear spin and not to possible higher-order multipole radiation as had been suggested [2]. Thus both the S and J labels are only nominal here. Bowen's conclusion was confirmed in 1937 by Mrozowski [3], who experimentally observed the $6s^2\,^1S_0$–$6s6p\,^3P_0$ line at 2656 Å in Hg I. This transition would be rigorously forbidden to all multipole orders of single-photon decay in an atom with a spinless nucleus by the $J=0\not\to J=0$ selection rule of angular-momentum conservation. Mrozowski [3] attributed the appearance of this line to coupling between the magnetic moments of the spin and orbit of the electron and the spin of the nucleus. A discussion of these transitions in Mg, Zn, Cd, and Hg has been given by Garstang [4].

In the two-electron case of the helium isoelectronic sequence, the existence of the $1s2s\,^3S_1$–$1s2p\,^3P_0$ $E1$ transition provides a decay channel not available to the alkaline-earth sequences. Thus the presence or absence of the hyperfine quenched $1s^2\,^1S_0$–$1s2p\,^3P_0$ channel can be detected in the triplet-to-triplet channel because the $^3P_0$ level has a lifetime that is sensitive to the nuclear spin.

Hyperfine quenching in the helium isoelectronic sequence was first observed by Gould, Marrus, and Mohr [5] who found that hyperfine effects contributed appreciably to the lifetime of the $2\,^3P_2$ level in V^{21+}. Calculations of decay rates for the $2\,^3P_0$ level in odd-Z nuclei $Z=9$ through $Z=29$ have been made by Mohr [6]. Recently, Marrus *et al.* [7] exploited the effect of hyperfine mixing to provide a determination of the $2\,^3P_1$–$2\,^3P_0$ fine-structure splitting in heliumlike Ag^{45+}, based on extensive calculations presented by Indelicato, Parente, and Marrus [8]. This experiment is significant because the mixed levels are nearly degenerate, and the method provides a sensitive means for measuring this energy splitting.

In this paper we report a direct observation of the effect of hyperfine quenching by comparing the lifetimes of $n=2$ decays in the two isotopes ^{61}Ni and ^{58}Ni. The isotope ^{58}Ni has nuclear spin $I=0$ and so will not be affected by hyperfine quenching, whereas ^{61}Ni has $I=\frac{3}{2}$, and hyperfine effects are important to understanding the lifetimes of the excited states. By using theoretical values for the lifetimes of the unperturbed levels and the matrix elements of the perturbation, our measurement of the quenched lifetime can be used to determine the $2\,^3P_0$–$2\,^3P_1$ level splitting. Alternatively, since the nickel measurement is not as sensitive to the fine-structure splittings as is the Ag^{45+} measurement of Marrus *et al.* [7], our results can be used to confirm the theory of the unquenched lifetimes and hyperfine-mixing matrix elements assuming the energy splittings are known. In this way, our work complements the Ag^{45+} work.

Figure 1 shows the low-lying atomic energy levels [9] of heliumlike Ni^{26+} and their theoretical lifetimes. The $2\,^1P_1$ and $2\,^3P_1$ levels are mixed by the spin-orbit interaction and decay primarily to the ground state by allowed $E1$ transitions [10]. All other levels in the spinless ^{58}Ni isotope decay by higher multipole radiation or by two-photon emission and so are relatively long lived. Hyperfine quenching in the isotope ^{61}Ni mixes the metastable levels $2\,^3P_2$ and $2\,^3P_0$ with the short-lived $2\,^3P_1$ and $2\,^1P_1$ states. Munger [11] has calculated the quenched lifetimes for the $2\,^3P_2$ hyperfine levels. The $F=\frac{7}{2}$ level is unperturbed and so has the same lifetime (71.0 ps) as the $2\,^3P_2$ level in $^{58}Ni^{26+}$. The $F=\frac{5}{2}$, $\frac{3}{2}$, $\frac{1}{2}$ levels have lifetimes of 69.7, 70.0, and 70.7 ps, respectively, and are only slightly affected by hyperfine quenching. Our experiment

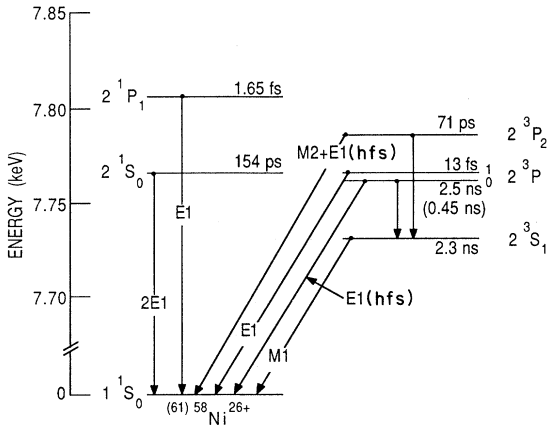

FIG. 1. Electronic energy-level diagram for the low-lying levels of heliumlike Ni^{26+} showing decay modes and lifetimes. E_1(hfs) refers to transitions in $^{61}Ni^{26+}$ induced by the hyperfine interaction. The $2\,^3P_0$ level has a lifetime of 2.5 ns in $^{58}Ni^{26+}$ and 0.45 ns in $^{61}Ni^{26+}$.

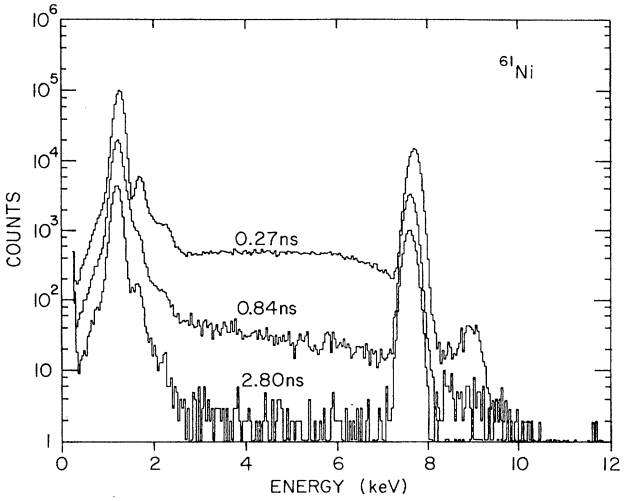

FIG. 2. Si(Li) detector spectra for three different foil-detector distances corresponding to times since excitation of 0.27, 0.84, and 2.8 ns.

is not sensitive to these small changes. On the other hand, there is a substantial effect on the lifetime of the $2\,^3P_0$ level. The theoretical lifetime [5] for this state is 2.5 ns in ^{58}Ni, while in ^{61}Ni values of 0.443 ns [11], 0.450 ns [12], and 0.464 ns [13] have been obtained. The difference between ^{58}Ni and ^{61}Ni is readily observed in our experiment.

The highly ionized nickel beams were obtained from the Argonne Tandem Linac (ATLAS). The ion source was charged with enriched isotopes of ^{61}Ni (42 at. %) and ^{58}Ni (58 at. %). First the Linac was tuned with the ^{58}Ni isotope for a beam energy of 340 MeV. The ions were prestripped with a 200-μg/cm^2 carbon foil, and the 26+ charge state (15% of the beam) was magnetically analyzed and directed to the experimental area. The switch to the ^{61}Ni isotope was accomplished by increasing the Tandem energy so the velocity of the ions delivered to the linac was the same as it was for ^{58}Ni. In this way, the linac parameters remained substantially the same, and in particular, the final velocity of the ions was the same for both isotopes. The velocity of the ions was determined with an uncertainty of 0.1% by a time-of-flight velocity analyzer. Since this analyzer was between the linac and the 200-μg/cm^2 foil, a correction had to be made for the energy loss in the foils. The final uncertainty in the velocity determination was 0.5%. The time-of-flight measurements verified that the velocity was the same for the two isotopes within this error.

In the experimental area a thin (42 μg/cm^2) carbon foil was moved relative to two fixed Si(Li) x-ray detectors, which were collimated so as to observe a region of 5 mm along the beam. The foil was mounted to a precision translation stage which measured the position to an accuracy of 10 μm. Decay curves were obtained by recording spectra as a function of foil-detector distance. A lower resolution silicon x-ray detector was attached to the target holder and used for normalization. It was collimated so as to observe a region along the beam axis from 5 to 15 mm from the target.

Spectra from one of the Si(Li) detectors are shown in Fig. 2 for three different foil-detector distances corresponding to delay times after excitation of 0.27, 0.84, and 2.8 ns. Prominent features include peaks at 7.8 and 1.4 keV and a broad continuum in between. There are also smaller peaks to the high-energy side of the intense peaks. The 1.4-keV peak corresponds to transitions from $n=3$ to 2 in lithiumlike and heliumlike ions. The broad continuum is largely due to the two-photon decays of the $2\,^1S_0$ level in heliumlike ions [14]. This component has a lifetime of 154 ps and is absent in the 2.8-ns spectrum. Of most interest for the present work is the 7.8-keV line. Apart from a small contribution due to cascade repopulation of the short-lived $2\,^3P_1$ and $2\,^1P_1$ levels, this line consists of a blend of transitions from the $2\,^3P_2$, $2\,^3P_0$, and $2\,^3S_1$ levels. The linewidth, which is dominated by the intrinsic resolution of the Si(Li) detectors (about 220 eV), is insufficient to resolve the individual transitions. At later delay times, the line narrows slightly and shifts to lower energy. This is due to depletion of the somewhat faster decaying $2\,^3P_2$ level, which lies 55 eV higher in energy than the $2\,^3S_1$ level.

The number of counts in the 7.8-keV line for the two Si(Li) detectors and the normalization detector are determined at each foil-detector distance by fitting them to a Gaussian plus a linear background. The width and position are taken as free parameters in order to allow for the fact that the line is a blend of transitions from states with different lifetimes. We then multiply the Si(Li) detector counts at each foil position by a factor that is the average normalization count divided by the normalization count at that position. The resulting normalized decay curves for one of the two Si(Li) detectors are shown in Fig. 3. The upper plot is the decay curve for the case of the spinless ^{58}Ni. These data are fitted well by two exponentials and a constant background. The short-lived component is identified with the $M2$ decay of the $2\,^3P_2$ state. From

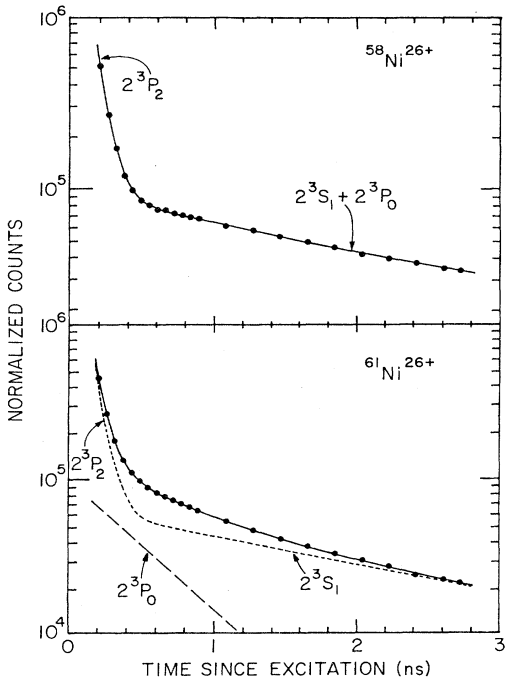

FIG. 3. Decay curves showing normalized count rate vs time since excitaiton for $^{58}Ni^{26+}$ (upper) and $^{61}Ni^{26+}$ (lower). The solid lines are the fits to the data. The dashed lines show contributions to the fit from the $2\,^3P_0$ level and the $2\,^3P_2+2\,^3S_1$ levels.

the fits to the data from the two detectors, we obtain a lifetime of 70(3) ps for this state in agreement with the theoretical values of Munger [11] (71 ps) and Gould, Marrus, and Mohr [5] (72 ps). The other component in the ^{58}Ni decay curve has contributions from both the $2\,^3S_1$ and the $2\,^3P_0$ states. The lifetimes of these states are 2.3 and 2.5 ns, respectively, and they are too close to be resolved as separate components. Although a good fit is obtained and the resulting lifetime for this component is consistent with the theoretical lifetimes, the ambiguity of the two contributions makes it difficult to make an accurate determination of either the unquenched $2\,^3P_0$ lifetime or the $2\,^3S_1$ lifetime.

The decay curve for the ^{61}Ni isotope, which was taken under identical conditions, shows a significant difference in shape compared to that of the ^{58}Ni data and does not fit to two exponentials (the reduced χ^2 for a two-exponential fit is 9.8). In order to fit these data, three exponentials are needed. Since our ^{58}Ni data confirm the theoretical value for the lifetime of the $2\,^3P_2$ level and recent data have confirmed agreement with theoretical values for the $2\,^3S_1$ lifetime [15,16], we base our determination of the lifetime of the $2\,^3P_0$ state in ^{61}Ni on a five-parameter fit. The five parameters are the amplitudes for the three exponentials, the lifetime of the $2\,^3P_0$ level and a constant background. The lifetimes of the $2\,^3P_2$ and $2\,^3S_1$ levels are fixed at the theoretical values. This fit is shown as the solid line in the lower plot of Fig. 3, and it is in excellent agreement with the data. Also shown in the lower part of Fig. 3 is the fitted curve with the $2\,^3P_0$ component left out. The shape of this curve is close to that of the ^{58}Ni data. The values for the $2\,^3P_0$ lifetime in ^{61}Ni obtained from these fits agree for the two detectors and so we simply average the two values to obtain 470(50) ps. We also tried fitting the data with other fitting procedures, including repeating the fit to three exponentials but allowing the $2\,^3P_2$ and $2\,^3S_1$ lifetimes to be free parameters. All of the fits are consistent with the results of the five-parameter fits which we chose for our final results. The quoted error in the determination of the $2\,^3P_0$ lifetime has been increased in order to account for the uncertainty inherent in using a many-component fitting function. Errors from cascade contributions are estimated to be less than 1%.

Our results for the quenched lifetime of the $2\,^3P_0$ level in $^{61}Ni^{26+}$ are in agreement with the various purely theoretical calculations [11,12,13] and provide confirmation of the theory for the unquenched lifetimes, mixing matrix elements, and energy levels. Another way to interpret the data, suggested by the work of Marrus *et al.* [7], is to use theoretical values for the matrix elements and unquenched lifetimes and use the experimental data to determine the $2\,^3P_0-2\,^3P_1$ fine-structure splitting $|\Delta E_{0-1}|$. Using the matrix elements and level widths calculated by Indelicato [13] and the procedure described in Ref. 7, we find that our value for the quenched lifetime 470(50) ps corresponds to a fine-structure splitting of $|\Delta E_{0-1}|=2.33(15)$ eV. This is in good agreement with the calculation of Drake [9] which yields 2.3090 eV.

We wish to acknowledge the excellent technical support provided by the ATLAS staff and by B. J. Zabransky during this experiment. This work was supported by the U.S. Department of Energy, Office of Basic Energy Sciences, under Contract Nos. W-31-109-ENG-38 and DE-FG05-88ER-13958 (University of Toledo) and by the National Science Foundation (Texas A&M University).

[1] I. S. Bowen (unpublished). See Ref. [2].
[2] D. Huff and W. V. Houston, Phys. Rev. **36**, 842 (1930).
[3] S. Mrozowski, Z. Phys. **108**, 204 (1938).
[4] R. H. Garstang, J. Opt. Soc. Am. **52**, 845 (1962).
[5] H. Gould, R. Marrus, and P. J. Mohr, Phys. Rev. Lett. **33**, 676 (1974).
[6] P. J. Mohr, in *Beam-Foil Spectroscopy*, edited by I. A. Sellin and D. J. Pegg (Plenum, New York, 1976), Vol. 1, p. 97.
[7] R. Marrus, A. Simionovici, P. Indelicato, D. D. Dietrich, P. Charles, J.-P. Briand, K. Finlayson, F. Bosch, D. Liesen, and F. Parente, Phys. Rev. Lett. **63**, 502 (1989).
[8] P. Indelicato, F. Parente, and R. Marrus, Phys. Rev. A **40**, 3505 (1989).
[9] G. W. F. Drake, Can. J. Phys. **66**, 586 (1988).
[10] C. D. Lin, W. R. Johnson, and A. Dalgarno, Phys. Rev. A

15, 154 (1977).
[11] C. T. Munger (private communication).
[12] Our own calculation, based on the formulation of Ref. [6] and the energy-level calculations given in Ref. [9].
[13] P. Indelicato, private communication. In the notation of Ref. [7], the matrix elements and level widths for $^{61}Ni^{26+}$ are given by $W_{11}=-0.0109$ eV, $W_{10}=-0.0057$ eV, $\Gamma_0=2.640\times10^{-7}$ eV, $\Gamma_1=0.0518$ eV.
[14] R. W. Dunford, M. Hass, E. Bakke, H. G. Berry, C. J. Liu, M. L. A. Raphaelian, and L. J. Curtis, Phys. Rev. Lett. **62**, 2809 (1989).
[15] R. Marrus, P. Charles, P. Indelicato, L. de Billy, C. Tazi, J.-P. Briand, A. Simionovici, D. D. Dietrich, F. Bosch, and D. Liesen, Phys. Rev. A **39**, 3725 (1989).
[16] R. W. Dunford, D. A. Church, C. J. Liu, H. G. Berry, M. L. A. Raphaelian, M. Hass, and L. J. Curtis, Phys. Rev. A **41**, 4109 (1990).